

# Fluctuations Indicate Strong Interlayer Coupling in Cuprate Superconductors

John A. Skinta and Thomas R. Lemberger

*Department of Physics, Ohio State University, Columbus, OH 43210-1106*

E. Wertz, K. Wu, and Q. Li

*Department of Physics, Pennsylvania State University, University Park, PA 16802*

(November 20, 2018)

From study of the Kosterlitz-Thouless-Berezinskii (KTB) transition in the superfluid density,  $n_s(T)$ , of ultrathin  $c$ -axis oriented  $\text{YBa}_2\text{Cu}_3\text{O}_{7-\delta}$  (YBCO) films, we find that interlayer coupling is unexpectedly strong. The KTB transition occurs at a high temperature, as if the films were isotropic rather than quasi-two-dimensional. This result agrees with a comparison of the superfluid density of YBCO with  $\text{Bi}_2\text{Sr}_2\text{CaCu}_2\text{O}_8$  and with numerical simulations of Josephson junction arrays, and challenges the thermal phase fluctuation interpretation of critical behavior near  $T_c$  in YBCO.

PACS numbers: 74.25.Fy, 74.40.+k, 74.76.Bz, 74.72.Bk

## I. INTRODUCTION

Studies of thermal fluctuations in the phase of the superconducting order parameter have a long history due to their importance in understanding phase transitions in general. Because of the high superfluid densities,  $n_s$ , and long coherence lengths,  $\xi$ , of conventional superconductors, fluctuations in three-dimensional (3D) samples are significant only within a hopelessly narrow temperature range near  $T_c$  [1], and most experimental studies involve thin amorphous films in which reduced dimensionality and superfluid density enhance fluctuations to an observable level. Two points that are relevant to work on fluctuations in high- $T_c$  cuprate superconductors have been established. First, quantum mechanical effects suppress thermal phase fluctuations (TPF's) when  $T$  drops below a surprisingly high temperature [2–4]. Second, at high temperatures where fluctuations are classical, simulations of Josephson junction (JJ) arrays [5] are in reasonable quantitative agreement with measurements of the superfluid density in two-dimensional (2D) films [2]. In this paper we concern ourselves with fluctuations in hole-doped cuprate superconductors in zero applied magnetic field.

Thermal phase fluctuations were immediately expected to be significant in cuprate superconductors [1], which have low superfluid densities and weak interlayer coupling. Exactly how important TPF's are is a matter of considerable debate. In the absence of directly comparable experimental results on quasi-2D conventional superconductors, we rely on simulations of strongly anisotropic JJ arrays [6] to provide a framework for examining experimental results. In  $\text{YBa}_2\text{Cu}_3\text{O}_{7-\delta}$  (YBCO), strong fluctuations are evidenced by very rapid changes in the  $ab$ -plane penetration depth  $\lambda(T)$  [7–9], specific heat [10], and coefficient of thermal expansion [11] over a 5 to 10 K interval near  $T_c$ . Perhaps the most striking evidence that these phenomena are due to TPF's is power-law behavior with the 3D-XY exponent  $2/3$  in the superfluid density,  $n_s(T) \propto \lambda^{-2}(T)$ , of YBCO crystals [7–9]. In the TPF interpretation, fluctuations are strong because of quasi-two-dimensionality, and interlayer coupling – although weak – begets a crossover from 2D to the observed 3D fluctuations [6,12].

Why not just accept these results at face value and move on? The reason is that  $T_c$  marks a second order phase transition from an unusual normal state to a  $d$ -wave superconductor. It would not be surprising if normal-state peculiarities persisted into the superconducting state and resulted in anomalous  $T$ -dependence of  $n_s$ . For example, if there is a normal-state order parameter (e.g., see Ref. 13), it may compete with the superconducting order parameter [14].

In the present paper, we argue from measurements of  $n_s$  in the literature and new measurements presented below, that TPF effects are actually small, presumably because interlayer coupling in cuprates is much stronger than indicated by transport measurements.

The pivotal notions of the TPF model are that fluctuations are strong because interlayer coupling is very weak, and that interlayer coupling serves only to change the  $T$ -dependence of  $n_s(T)$  from a discontinuous Kosterlitz-Thouless-Berezinskii (KTB) [15] drop at  $T_{KT B}^*$  to a continuous decrease to zero, with rapidly increasing downward curvature [6,12]. One key quantity in comparing  $n_s(T)$  with the TPF model is the hypothetical transition temperature,  $T_{KT B}^*$ , at which the KTB transition would occur if layers could be completely decoupled without affecting the pairing

interaction.  $T_{KTB}^*$  can be deduced from the measured  $ab$ -plane superfluid density. A quantitative measure of the strength of fluctuations, and therefore of interlayer coupling, is the difference between  $T_{KTB}^*$  and the temperature,  $T_c$ , at which  $n_s(T)$  vanishes: the weaker the coupling, the smaller the difference. From numerical results in Ref. 6,  $T_c/T_{KTB}^* - 1$  increases roughly as  $(J_\perp/J_\parallel)^{1/3}$ , where  $J_\perp$  ( $J_\parallel$ ) is the interlayer (intralayer) coupling strength. The other key quantity is  $n_s(T_{KTB}^*) \propto \lambda^{-2}(T_{KTB}^*)$ . In the TPF model, 3D-XY critical behavior develops only as  $n_s$  approaches zero, i.e., for  $n_s(T) \ll n_s(T_{KTB}^*)$ .

Let us now take a closer look at power-law behavior in  $n_s(T)$  observed for some YBCO samples, setting aside concerns that power-law behavior is not seen in other YBCO samples [16,17] nor in clean  $\text{Bi}_2\text{Sr}_2\text{CaCu}_2\text{O}_8$  (BSCCO) crystals [18]. A recent measurement of the  $a$ -axis magnetic penetration depth in a clean, optimally doped YBCO crystal [9] finds that at temperatures from  $\sim 85\%$  to  $\sim 99.9\%$  of the transition at  $T_c \approx 93.78$  K,  $\lambda_a^{-2}(T)$  is fitted to within a percent or so by  $\lambda_a^{-2}(T)/\lambda_a^{-2}(0) \approx 1.26(1 - T/T_c)^{2/3}$ . The critical region encompasses a remarkably large range of temperature and superfluid density:  $0.85 \leq T/T_c \leq 0.999$  and  $0.01 \leq \lambda_a^{-2}(T)/\lambda_a^{-2}(0) \leq 0.35$ . The argument that an excellent fit is unlikely to be accidental is taken as support for the TPF model, but in reality it is not. The reason is that in the TPF model the crossover from 3D to 2D fluctuations occurs well inside the observed “critical region”. To see this, let us estimate  $T_{KTB}^*$  and  $\lambda_a^{-2}(T_{KTB}^*)$  from the data. With an effective layer thickness equal to the center-to-center spacing between  $\text{CuO}_2$  bilayers ( $d = 1.17$  nm),  $\lambda_a(0) = 160$  nm, and the KTB prediction [15]

$$\lambda_\perp^{-1}(T_{KTB}) = \frac{T_{KTB}}{9.8 \text{ mmK}}, \quad (1)$$

where  $\lambda_\perp^{-1} \equiv d\lambda^{-2}$ , we find  $T_{KTB}^* \approx 0.96T_c$  and  $\lambda_a^{-2}(T_{KTB}^*) \approx \lambda_a^{-2}(0)/7$ . The TPF model predicts 3D-XY behavior only for  $\lambda^{-2}(T) \ll \lambda^{-2}(T_{KTB}^*)$ , which for these data means  $T \geq 0.99T_c$ . Power-law behavior from 0.85 to 0.99  $T_c$  would have to be “accidental”. Taking this one step further, if power-law behavior is due to physics beyond the TPF model, then TPF’s must be so weak as to be unapparent in the data.

Another argument against the TPF model arises from comparison of YBCO with BSCCO, which has  $\text{CuO}_2$  bilayers that are nearly identical structurally to those of YBCO – i.e., the same interplanar spacing and nearly square Cu-O structure – except that  $\text{Y}^{3+}$  is replaced by  $\text{Ca}^{2+}$  [19]. As expected, the areal superfluid density,  $n_s(T)d$ , at  $T = 0$  of the bilayers in clean BSCCO is essentially the same as in the  $a$ -axis direction (perpendicular to  $\text{CuO}$  chains) in YBCO. However, BSCCO has interlayer coupling several hundred times weaker than YBCO, as measured by transport [20,21], so we expect TPF’s to be much stronger. Let us see.  $T_c$  lies 4 K above  $T_{KTB}^*$  in YBCO crystals, as found above – a reasonable result when compared with simulations of JJ arrays [6]. In BSCCO, the difference is 10 K, indicating that fluctuations in BSCCO are actually weaker than in YBCO. The latter number comes from clean BSCCO crystals [18] in which  $\lambda^{-2}(T)$  decreases linearly with  $T$  at low  $T$ ,  $T_c$  is 91 K, the center-to-center spacing between  $\text{CuO}_2$  bilayers is 1.54 nm [19], and  $\lambda(0) = 210$  nm. Evidently interlayer coupling is stronger in BSCCO than indicated by transport measurements of  $ab$ -plane *vs.*  $c$ -axis anisotropy.

We could refine the above estimations by using two interlayer coupling constants, one within bilayers and another between bilayers, per Carlson *et al.* [6], and use an average of the  $ab$ -plane superfluid density rather than just the  $a$ -axis value in YBCO, but the conclusions do not change.

Other experimental evidence supports the proposition that interlayer coupling is stronger than expected. Some corroboration is provided by a study of  $\sigma_1(\omega, T)$  above  $T_c$  in YBCO crystals [8], which finds a critical region of only 0.6 K. More direct support is provided by the measurements presented below, which demonstrate that fluctuation effects in the 2D penetration depth,  $\lambda_\perp^{-1}(T) \propto n_s(T)d$ , of ultrathin twinned YBCO films ( $d = 4, 8$ , and 10 unit cells) are quantitatively consistent with measurements on 2D  $s$ -wave films [2,22], assuming that the YBCO films are effectively isotropic – i.e., that their layers are strongly coupled.

## II. EXPERIMENTAL

The films examined in this study were grown epitaxially by pulsed laser deposition on  $\text{NdGaO}_3$  substrates, as detailed elsewhere [23]. Each  $1 \text{ cm} \times 1 \text{ cm}$  film consists of buffer layers of semiconducting  $\text{Pr}_{0.6}\text{Y}_{0.4}\text{Ba}_2\text{Cu}_3\text{O}_{7-\delta}$  that are 12 unit cells thick above, and 8 unit cells thick below, the YBCO film. The underlayer lessens the strain of substrate lattice mismatch on the YBCO, while the capping layer protects the ultrathin YBCO film from damage during handling. The three films we examined are nominally 4, 8, and 10 unit cells thick; however, it is likely that the top and bottom unit-cell layers are not perfectly smooth or homogeneous, leading to some uncertainty in the film thickness  $d$ . We therefore estimate  $d = 4 \pm 1, 8 \pm 1$ , and  $10 \pm 1$  unit cells for the three films.

We measure  $\lambda_\perp^{-1}(T)$  with a two-coil mutual inductance technique described in detail elsewhere [24]. The films are centered between two counterwound coils approximately 2 mm in diameter and 1 mm long. In a typical measurement,

the sample is cooled to liquid helium temperatures, and a current of 100  $\mu\text{A}$  is driven at 50 kHz through the coil pressed against the back of the substrate. The supercurrents created in the sample are very nearly uniform through the film thickness. Thus, we observe the  $T_c$ 's of all layers in the film. As the temperature slowly increases, the voltage induced in the secondary coil, which is pressed against the film, is measured continuously. The complex sheet conductivity  $\sigma(\omega, T)d = \sigma_1(\omega, T)d - i\sigma_2(\omega, T)d$  of the *entire* film is deduced directly from the measured mutual inductance. The 2D penetration depth is obtained with an accuracy of about 3% from the imaginary part of the sheet conductivity from  $\lambda_{\perp}^{-1}(T) \equiv \mu_0\omega\sigma_2(T)d$ , where  $\mu_0$  is the permeability of vacuum. The uncertainty in film thickness enters only into calculation of the 3D penetration depth  $\lambda^{-2}(T)$ , and into the 2D penetration depth of *each* unit-cell layer.

Figure 1 displays  $\lambda_{\perp}^{-1}(T)$  as measured at 50 kHz for each film at optimal doping. An accelerated decrease in  $\lambda_{\perp}^{-1}$  at high temperatures is most obvious for the 4 unit cell film, but similar features are apparent very close to  $T_c$  for the 8 and 10 unit-cell films as well. The transitions are slightly broader than in *a*-MoGe films [2], presumably due to slight inhomogeneity. The vertical dotted lines mark the location of the peak in  $\sigma_1(50 \text{ kHz}, T)$ , whose temperature we define to be  $T_c$  and which very nearly coincides with the predicted KTB transition temperature,  $T_{KTB}$ , for an isotropic film. To further motivate association of the drop in  $\lambda_{\perp}^{-1}(T)$  with the KTB transition, we appeal to the frequency dependences of  $\sigma_1$  and  $\lambda_{\perp}^{-1}$  near the transition. Without going into detail, the observed shift of  $\sigma_1$  and  $\lambda_{\perp}^{-1}$  to higher temperature with increasing frequency, shown in Fig. 2 for the 10 unit cell film, is quite similar to behavior seen in *a*-MoGe films [22]. The experimental  $T_c$  in these ultrathin films marks a KTB transition.

Arrows in Fig. 1 indicate  $T_{KTB}^*$  – the KTB transition temperature for uncoupled layers – showing that  $T_{KTB}^*$  lies 8 to 20 K below  $T_c$ , a difference significantly larger than seen in YBCO crystals [7–9] and simulations of JJ arrays [6]. Another indicator of fluctuation effects is a rapid increase in downward curvature of  $\lambda_{\perp}^{-1}$  for  $T > T_{KTB}^*$  as predicted by the TPF model. The thin solid curves in Fig. 1 are extrapolations of quadratic fits to the data over  $T_{KTB}^* - 10 \text{ K} \leq T \leq T_{KTB}^*$ . We emphasize that the quadratics fit the data extremely well over at least 20 K below  $T_{KTB}^*$ , highlighting the constant curvature of the data below  $T_{KTB}^*$ . The insets to Fig. 1 show that only as  $T$  gets close to  $T_c$  is a change in curvature of the data apparent. The proximity of the accelerated drops in  $\lambda_{\perp}^{-1}$  to the predicted  $T_{KTB}$ , and the lack of fluctuation effects (e.g., strong downward curvature) at  $T_{KTB}^*$ , indicate the presence of strong interlayer coupling.

We now address an important quantitative issue: the suppression of  $\lambda_{\perp}^{-1}$  below its mean-field value just below  $T_{KTB}$ . Taking the thin solid curves in Fig. 1 as reasonable estimates of the mean-field behavior of  $\lambda_{\perp}^{-1}$ , we conclude that  $\lambda_{\perp}^{-1}$  is 35% to 75% of its mean-field value at the transition, in agreement with results from *a*-MoGe films [2] and calculations for 2D JJ arrays [5].

Thus, the fluctuation behavior of ultrathin YBCO films is quantitatively similar to that of *a*-MoGe films. Within the TPF model, the only explanation is that interlayer coupling in the YBCO films is much stronger than expected from transport anisotropy. The strong *ab*-plane *vs.* *c*-axis anisotropy in transport coefficients could be explained phenomenologically by occasional weak links between adjacent  $\text{CuO}_2$  bilayers, with most bilayers coupled strongly to their neighbors.

### III. CONCLUSION

We have presented high precision, low frequency measurements of  $\lambda_{\perp}^{-1}(T)$  and  $\sigma_1(T)$  in YBCO films of 4 to 10 unit cells thickness. The data indicate that interlayer coupling is strong, insofar as thermal phase fluctuations are concerned. Whatever the origin of the coupling, it is the presence of an additional layer or layers that lessens the effect of fluctuations on a single unit-cell layer. These results, and literature results for the *ab*-plane superfluid density of BSCCO crystals, argue that fluctuations are much weaker in cuprates than one would expect based on anisotropic transport coefficients. The power-law behavior near  $T_c$  seen in the superfluid density of very clean YBCO crystals – cited as evidence of strong thermal phase fluctuations – is due to some other physics, perhaps competition between the superconducting order parameter and a normal-state order parameter that is sensitive to disorder. The idea of a normal-state order parameter has been proposed on various grounds [13,14]. The theory of Rokhsar [14] suggests that the critical region may be more complicated than in the usual superconducting-to-normal transition when the normal and superconducting order parameters interact.

#### IV. ACKNOWLEDGEMENTS

The authors gratefully acknowledge useful discussions with C. Jayaprakash and Y.-B. Kim. This work was supported in part by DoE Grant DE-FG02-90ER45427 through the Midwest Superconductivity Consortium.

---

- [1] C.J. Lobb, Phys. Rev. B **36**, 3930 (1987).
- [2] S.J. Turneaure, T.R. Lemberger, and J.M. Graybeal, Phys. Rev. Lett. **84**, 987 (2000).
- [3] T.R. Lemberger, A.A. Pesetski, and S.J. Turneaure, Phys. Rev. B **61**, 1483 (2000).
- [4] L. Benfatto, S. Caprara, C. Castellani, A. Paramekanti, and M. Randeria, Phys. Rev. B **63**, 174513 (2001).
- [5] T. Ohta and D. Jasnow, Phys. Rev. B **20**, 139 (1979); S. Teitel and C. Jayaprakash, Phys. Rev. Lett. **51**, 1999 (1983); Phys. Rev. B **27**, 598 (1983); W.Y. Shih and D. Stroud, *ibid.* **32**, 158 (1985); I.-J. Hwang and D. Stroud, *ibid.* **57**, 6036 (1998).
- [6] E.W. Carlson, S.A. Kivelson, V.J. Emery, and E. Manousakis, Phys. Rev. Lett. **83**, 612 (1999).
- [7] S. Kamal, D.A. Bonn, N. Goldenfeld, P.J. Hirschfeld, R. Liang, and W.N. Hardy, Phys. Rev. Lett. **73**, 1845 (1994).
- [8] S.M. Anlage, J. Mao, J.C. Booth, D.H. Wu, and J.L. Peng, Phys. Rev. B **53**, 2792 (1996).
- [9] S. Kamal, R. Liang, A. Hosseini, D.A. Bonn, and W.N. Hardy, Phys. Rev. B **58**, R8933 (1998).
- [10] M. Charalambous, O. Riou, P. Gandit, B. Billon, P. Lejay, J. Chaussy, W.N. Hardy, D.A. Bonn, and R. Liang, Phys. Rev. Lett. **83**, 2042 (1999).
- [11] V. Pasler, P. Schweiss, C. Meingast, B. Obst, H. Wühl, A.I. Rykov, and S. Tajima, Phys. Rev. Lett. **81**, 1094 (1998).
- [12] T. Schneider and J.M. Singer, Physica (Amsterdam) **341-348C**, 87 (2000).
- [13] S. Chakravarty, R.B. Laughlin, D.K. Morr, and C. Nayak, Phys. Rev. B **63**, 094503 (2001).
- [14] D.S. Rokhsar, Phys. Rev. Lett. **70**, 493 (1993).
- [15] J.M. Kosterlitz and D.J. Thouless, J. Phys. C **6**, 1181 (1973); J.M. Kosterlitz, *ibid* **7**, 1046 (1974); V.L. Berezinskii, Sov. Phys. JETP **32**, 493 (1971).
- [16] H. Srikanth, Z. Zhai, S. Sridhar, A. Erb, and E. Walker, Phys. Rev. B **57**, 7986 (1998).
- [17] K.M. Paget, B.R. Boyce, and T.R. Lemberger, Phys. Rev. B **59**, 6545 (1999).
- [18] S.-F. Lee, D.C. Morgan, R.J. Ormeno, D.M. Broun, R.A. Doyle, J.R. Waldram, and K. Kadowaki, Phys. Rev. Lett. **77**, 735 (1996).
- [19] R.M. Hazen, in *Physical Properties of High Temperature Superconductors II*, edited by D.M. Ginsberg (World Scientific, Singapore, 1990).
- [20] Y. Iye, in *Physical Properties of High Temperature Superconductors III*, edited by D.M. Ginsberg (World Scientific, Singapore, 1992).
- [21] X.H. Chen, M. Yu, K.Q. Ruan, S.Y. Li, Z. Gui, G.C. Zhang, and L.Z. Cao, Phys. Rev. B **58**, 14219 (1998).
- [22] S.J. Turneaure, T.R. Lemberger, and J.M. Graybeal, Phys. Rev. B **63**, 174505 (2001).
- [23] C. Kwon, Q. Li, X.X. Xi *et al.*, Appl. Phys. Lett. **62**, 1289 (1993); C. Kwon, Q. Li, I. Takeuchi *et al.*, Physica (Amsterdam) **266C**, 75 (1996).
- [24] S.J. Turneaure, E.R. Ulm, and T.R. Lemberger, J. Appl. Phys. **79**, 4221 (1996); S.J. Turneaure, A.A. Pesetski, and T.R. Lemberger, *ibid.* **83**, 4334 (1998).

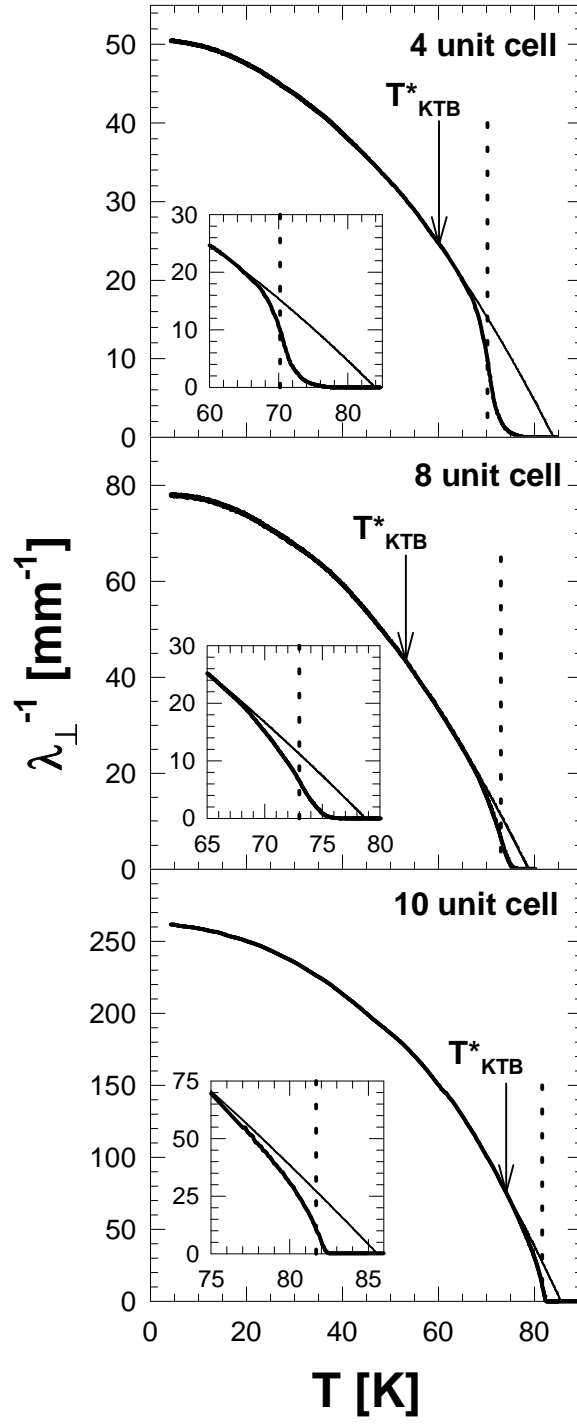


FIG. 1.  $\lambda_{\perp}^{-1}$  vs.  $T$  measured at 50 kHz for three ultrathin YBCO films at optimal doping (thick solid lines). The vertical dotted lines locate the positions of the peaks in  $\sigma_1(50 \text{ kHz}, T)$ , which very nearly coincide with  $T_{KT B}$ . The thin solid lines are extrapolated quadratic fits to  $\lambda_{\perp}^{-1}(T)$  over  $T_{KT B}^* - 10 \text{ K} \leq T \leq T_{KT B}^*$  and provide an estimate of the “mean-field” behavior of  $\lambda_{\perp}^{-1}$  for  $T \geq T_{KT B}^*$ . Insets are enlarged views of the transition regions.

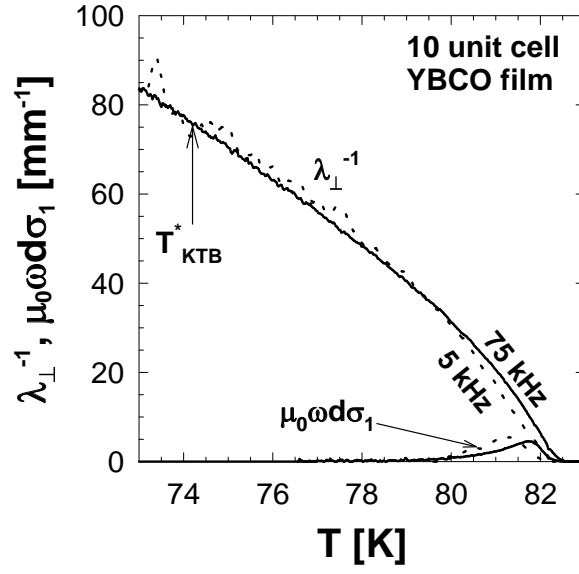


FIG. 2.  $T$  dependence of the 2D penetration depth,  $\lambda_{\perp}^{-1}$ , and conductivity,  $\mu_0\omega d\sigma_1$ , at 5 kHz (dotted lines) and 75 kHz (solid lines) for the 10 unit-cell-thick YBCO film. The arrow indicates  $T_{KTB}^*$ .